

Energy estimators for random series path-integral methods

Cristian Predescu, Dubravko Sabo, and J. D. Doll

Department of Chemistry, Brown University, Providence, Rhode Island 02912

David L. Freeman

Department of Chemistry, University of Rhode Island, Kingston, Rhode Island 02881

(Dated: January 28, 2020)

We perform a thorough analysis on the choice of estimators for random series path integral methods. In particular, we show that both the thermodynamic (T-m method) and the direct (H-m method) energy estimators have finite variances and are straightforward to implement. It is demonstrated that the agreement between the T-m method and the H-m method estimators provides an important consistency check on the quality of the path integral simulations. We illustrate the behavior of the various estimators by computing the total, kinetic, and potential energies of a molecular hydrogen cluster using three different path integral techniques. Statistical tests are employed to validate the sampling strategy adopted as well as to measure the performance of the parallel random number generator utilized in the Monte Carlo simulation. Some issues raised by previous simulations of the hydrogen cluster are clarified.

PACS numbers: 05.30.-d, 02.70.Ss

Keywords: Monte Carlo path integral methods, energy estimators, reweighted techniques

I. INTRODUCTION

Numerical path integral methods have proved to be highly useful tools in the analysis of finite temperature, many-body quantum systems.¹ A central theme in such studies is the conscious use of dimensionality, both in the reformulation of the original problem and in the subsequent numerical simulations.

As the scale of the problems under study continues to grow, it becomes increasingly important that the formal properties of the numerical methods that are utilized be properly characterized. Recently, Predescu and co-workers^{2,3,4} have presented a number of results concerning the convergence properties of random series-based path integral techniques. Important in their own right, these formal properties have also led to the development of a new class of path integral methods, the so-called reweighted techniques.⁴ Reweighted approaches accelerate the convergence of "primitive" series methods by including the effects of "higher-order" path variables in a simple, approximate fashion. Reweighted methods achieve the convergence rate of related partial averaging approaches⁵ without requiring the construction of the Gaussian transform of the underlying potential energy function.

Previous work on the reweighted method has focused principally on the construction of the quantum-mechanical density matrix.^{4,6} In the present work, we wish to examine estimators for various coordinate-diagonal and off-diagonal properties. While the present discussion is focused principally on reweighted methods, the results obtained are broadly applicable to more general random series approaches.

The remainder of the paper is organized as follows: Section II examines the thermodynamic (T-m method) and direct (H-m method) estimators for the total energy. To

minimize possible confusion, we note that as presented here the T-m method results emerge naturally in "virial"⁷ form and thus avoid the variance difficulties sometimes associated with such approaches.^{8,9} In Section III we examine the application of the reweighted methods to a model problem, that of simulating the thermodynamic properties of the (H₂)₂₂ molecular cluster. Finally, in Section IV we summarize our present findings and clarify a number of issues raised in previous studies of this molecular hydrogen system.^{10,11}

II. ENERGY ESTIMATORS

In this section, we consider a one-dimensional quantum canonical system characterized by inverse temperature $\beta = 1/(k_B T)$ and set forward the task of computing its average energy by Monte Carlo integration methods developed around several reweighted techniques.^{4,6} The physical system is made up of a particle of mass m_0 moving in the potential $V(x)$. We discuss the numerical implementation and the computational merits of both the T-m method and H-m method estimators. Any time the multidimensional extension is not obvious, we present the explicit formulas of the respective estimators.

We begin by presenting the general form of the path integral methods we employ in this paper. We remind the reader that in terms of a standard Brownian motion $fB_u; u \geq 0$, the Feynman-Kac formula has the expression¹²

$$E[x; x^0; \beta] = \int_{-\infty}^{\infty} \int_0^{\infty} e^{-\int_0^t V(B_u) du} \frac{1}{\sqrt{2\pi m_0}} B_1 = x^0; B_0 = x; \quad (1)$$

where $\beta = (\gamma^2 m_0)^{1/2}$. It is straightforward to see that the first factor of the product in Eq. (1) (which repre-

sents the conditional probability density that the rescaled Brownian motion B_u reaches the point x^0 provided that it starts at the point x , is the density matrix of a free particle of mass m_0

$$P[B_1 = x^0 | B_0 = x] = f_p(x; x^0; \cdot)$$

Moreover, rather than using the conditional expectation appearing in the second factor of Eq. (1), one usually employs a stochastic process $fB_u^0; 0 \leq u \leq 1$, called a standard Brownian bridge,^{12,13} which is defined as a standard Brownian motion conditioned on the end points such that $B_0^0 = 0$ and $B_1^0 = 0$. In terms of the newly defined process, the Feynman-Kac formula reads

$$\frac{(x; x^0; \cdot)}{f_p(x; x^0; \cdot)} = E \exp \int_0^1 V[x_r(u) + B_u^0] du ;$$

where $x_r(u) = x + (x^0 - x)u$ is a straight line connecting the points x and x^0 and is called the reference path.

As discussed in Ref. (2), one of the most general constructions of the standard Brownian bridge is given by the Ito-Nisio theorem.¹⁴ Let $f_k(\cdot)g_{k-1}$ be a system of functions on the interval $[0; 1]$, which together with the constant function $\delta(\cdot) = 1$, make up an orthonormal basis in $L^2[0; 1]$. Let

$$z_k(t) = \int_0^t g_k(u) du ;$$

If is the space of infinite sequences $a = (a_1; a_2; \dots)$ and

$$dP[\mathbf{a}] = \prod_{k=1}^{\infty} d(a_k) \quad (2)$$

is the probability measure on such that the coordinates a_k are independent identically distributed (i.i.d.) variables with distribution probability

$$d(a_i) = \frac{1}{\sqrt{2\pi}} e^{-a_i^2/2} da_i ; \quad (3)$$

then

$$B_u^0(a) \stackrel{d}{=} \sum_{k=1}^{\infty} a_k z_k(u); 0 \leq u \leq 1; \quad (4)$$

i.e., the right-hand side random series is equal in distribution to a standard Brownian bridge. The notation $B_u^0(a)$ in (4) is then appropriate and allows us to interpret the Brownian bridge as a collection of random functions of argument a , indexed by u .

Using the Ito-Nisio representation of the Brownian bridge, the Feynman-Kac formula takes the form

$$\frac{(x; x^0; \cdot)}{f_p(x; x^0; \cdot)} = dP[\mathbf{a}] \exp \int_0^1 V[x_r(u) + \sum_{k=1}^{\infty} a_k z_k(u)] du ; \quad (5)$$

For a multidimensional system, the Feynman-Kac formula is obtained by employing an independent random series $\sum_{k=1}^{\infty} a_k z_k(u)$ is any sequence of approximations to the density matrix of the form⁴

$$\frac{P^R(x; x^0; \cdot)}{f_p(x; x^0; \cdot)} = \prod_{k=1}^{\infty} \frac{d(a_k)}{d(a_{qn+p})} \exp \int_0^1 V[x_r(u) + \sum_{k=1}^{qn+p} a_k z_{n+k}(u)] du ; \quad (6)$$

where q and p are some fixed integers, where

$$z_{n+k}(u) = a_k(u) \text{ if } 1 \leq k \leq n; \quad (7)$$

and where

$$\sum_{k=n+1}^{qn+p} z_{n+k}(u)^2 = \sum_{k=n+1}^{qn+p} a_k^2(u); \quad (8)$$

It is convenient to introduce the additional quantities $X_n(x; x^0; a; \cdot)$ and $X_1(x; x^0; a; \cdot)$, which are defined by the expressions

$$X_n(x; x^0; a; \cdot) = \prod_{k=1}^n \frac{d(a_k)}{d(a_{qn+p})} \exp \int_0^1 V[x_r(u) + \sum_{k=1}^{qn+p} a_k z_{n+k}(u)] du \quad (9)$$

and

$$X_1(x; x^0; a; \cdot) = \prod_{k=1}^{\infty} \frac{d(a_k)}{d(a_{qn+p})} \exp \int_0^1 V[x_r(u) + \sum_{k=1}^{qn+p} a_k z_{n+k}(u)] du ; \quad (10)$$

respectively. With the new notation, Eq. (6) becomes

$$\frac{P^R(x; x^0; \cdot)}{f_p(x; x^0; \cdot)} = dP[\mathbf{a}] X_n(x; x^0; a; \cdot); \quad (11)$$

while the Feynman-Kac formula reads

$$(x; x^0; \cdot) = dP[\mathbf{a}] X_1(x; x^0; a; \cdot); \quad (12)$$

The analytical expressions of the functions $z_{n+k}(u)$ depend on the nature of the reweighted techniques and are generally chosen to maximize the asymptotic convergence of the respective reweighted techniques.⁴ To a large extent, the specific form of these functions is not important for the present development, but the reader is advised to consult Refs. (4) and (6) for quadrature techniques and additional clarifications.

The remainder of the present section is split into two parts. First, we discuss the problem of computing the ensemble averages of operators diagonal in coordinate representation. In particular, this resolves the problem of computing the average potential energy. Second, we consider the problem of evaluating the total energies (hence, also the kinetic energies) by means of the T-m method and H-m method estimators.

A. Operators diagonal in the coordinate representation

By definition, the ensemble average of an operator \hat{O} diagonal in the coordinate representation is

$$\text{hO } i = \frac{\int_R \int_R \langle x; x; \rangle O(x) dx}{\int_R \langle x; x \rangle dx} : \quad (13)$$

The quantity $\langle x; x; \rangle = \langle x; x; x \rangle$ is the diagonal density matrix. By convention, we drop the second variable of the pair $\langle x; x; \rangle$ any time $x = x^0$. For instance, we use $X_n(x; a; \cdot)$ instead of $X_n(x; x; a; \cdot)$. By means of Eq. (12), the average above can be recast as

$$\text{hO } i = \frac{\int_R \int_R \frac{dx}{R} \frac{dP}{R} \langle x; a; \rangle X_1(x; a; \cdot) O(x)}{\int_R \frac{dx}{R} \frac{dP}{R} \langle x; a; \rangle X_1(x; a; \cdot)} : \quad (14)$$

This average can be recovered as the limit $n \rightarrow 1$ of the sequence

$$\text{hO } i_{;n}^{\text{pt}} = \frac{\int_R \int_R \frac{dx}{R} \frac{dP}{R} \langle x; a; \rangle X_n(x; a; \cdot) O(x)}{\int_R \frac{dx}{R} \frac{dP}{R} \langle x; a; \rangle X_n(x; a; \cdot)} : \quad (15)$$

the terms of which are to be evaluated by Monte Carlo integration. The estimating function $O(x)$ appearing in the above formula is called the point estimating function of the operator \hat{O} .

An alternative to the point estimating function is the so-called path estimating function, the derivation of which is presented shortly. As demonstrated in Appendix A, the function $O(x)$ appearing in Eq. (14) can be replaced by $O[x + B_u^0(a)]$, without changing the value of the average $\text{hO } i$. That is, the equality

$$\text{hO } i = \frac{\int_R \int_R \frac{dx}{R} \frac{dP}{R} \langle x; a; \rangle X_1(x; a; \cdot) O[x + B_u^0(a)]}{\int_R \frac{dx}{R} \frac{dP}{R} \langle x; a; \rangle X_1(x; a; \cdot)}$$

is valid for all $0 \leq u \leq 1$. Averaging over the variable u , one obtains

$$\text{hO } i = \frac{\int_R \int_R \frac{dx}{R} \frac{dP}{R} \langle x; a; \rangle X_1(x; a; \cdot) \int_0^1 O[x + B_u^0(a)] du}{\int_R \frac{dx}{R} \frac{dP}{R} \langle x; a; \rangle X_1(x; a; \cdot)} : \quad (16)$$

Eq. (16) shows that the ensemble average of the operator \hat{O} can also be recovered as the limit $n \rightarrow 1$ of the sequence

$$\text{hO } i_{;n}^{\text{pth}} = \frac{\int_R \int_R \frac{dx}{R} \frac{dP}{R} \langle x; a; \rangle X_n(x; a; \cdot) \int_0^1 O[x + B_{u;n}^0(a)] du}{\int_R \frac{dx}{R} \frac{dP}{R} \langle x; a; \rangle X_n(x; a; \cdot)} : \quad (17)$$

where we have set

$$B_{u;n}^0(a) = \sum_{k=1}^{nR_1} a_k \tilde{\gamma}_{n;k}(u)$$

for convenience of notation.

In the remainder of the present subsection, we discuss the relative merits of the point and path estimators. We first consider which of $\text{hO } i_{;n}^{\text{pt}}$ and $\text{hO } i_{;n}^{\text{pth}}$ is closer to $\text{hO } i$ for a given n assuming the averages given in Eqs. (15) and (17) are computed exactly. Let us notice that Eq. (15) can be put in the form

$$\text{hO } i_{;n}^{\text{pt}} = \frac{\int_R \frac{dx}{R} \frac{dP}{R} \langle x; a; \rangle X_1(x; a; \cdot) O(x)}{\int_R \frac{dx}{R} \frac{dP}{R} \langle x; a; \rangle X_1(x; a; \cdot)} :$$

The probability distribution

$$\frac{\int_R \frac{dx}{R} \frac{dP}{R} \langle x; a; \rangle X_1(x; a; \cdot) O(x)}{\int_R \frac{dx}{R} \frac{dP}{R} \langle x; a; \rangle X_1(x; a; \cdot)} : \quad (18)$$

represents the marginal distribution of the variable x regarded as a random variable on the space R , which is endowed with the probability measure

$$\frac{\int_R \frac{dx}{R} \frac{dP}{R} \langle x; a; \rangle X_1(x; a; \cdot) O(x)}{\int_R \frac{dx}{R} \frac{dP}{R} \langle x; a; \rangle X_1(x; a; \cdot)} : \quad (19)$$

The reweighted techniques are designed so that the distribution given by Eq. (18) is as close as possible to the quantum statistical one, which is given by the expression

$$\frac{\int_R \frac{dx}{R} \frac{dP}{R} \langle x; a; \rangle X_1(x; a; \cdot) O(x)}{\int_R \frac{dx}{R} \frac{dP}{R} \langle x; a; \rangle X_1(x; a; \cdot)} :$$

In designing the reweighted techniques, one seeks to optimize the rate of convergence of the sequence $\langle x; x^0; \cdot \rangle ! \langle x; x^0; \cdot \rangle$ for all x and x^0 .

For arbitrary u , the marginal distribution of $x + B_{u;n}^0(a)$ is usually different from the one given by Eq. (18) and is not optimized. With few notable exceptions to be analyzed below, the points $x + B_{u;n}^0(a)$ for different u are not equivalent, and their probability distribution may differ significantly from the quantum statistical one. (However, as shown in Appendix A, they become equivalent in the limit $n \rightarrow 1$.) Therefore, especially for those reweighted techniques having fast asymptotic convergence, we expect the point estimator to be more rapidly convergent with n than the path estimator.

An additional issue appearing in Monte Carlo computations is the variance of the two estimating functions $O(x)$ and $\int_0^1 O[x + B_{u;n}^0(a)] du$. In the limit $n \rightarrow 1$, the variance of the point estimating function converges to

$$\begin{aligned} & \frac{\int_R \frac{dx}{R} \frac{dP}{R} \langle x; a; \rangle X_1(x; a; \cdot) O(x)^2}{\int_R \frac{dx}{R} \frac{dP}{R} \langle x; a; \rangle X_1(x; a; \cdot)} - \text{hO } i^2 \\ &= \frac{\int_R \frac{dx}{R} \frac{dP}{R} \langle x; a; \rangle X_1(x; a; \cdot) \int_0^1 O[x + B_u^0(a)]^2 du}{\int_R \frac{dx}{R} \frac{dP}{R} \langle x; a; \rangle X_1(x; a; \cdot)} - \text{hO } i^2 ; \end{aligned}$$

while the variance of the path estimating function converges to

$$\frac{\int_R \frac{dx}{R} \frac{dP}{R} \langle x; a; \rangle X_n(x; a; \cdot) \int_0^{nR_1} O[x + B_u^0(a)] du}{\int_R \frac{dx}{R} \frac{dP}{R} \langle x; a; \rangle X_n(x; a; \cdot)} - \text{hO } i^2 :$$

The Cauchy-Schwartz inequality implies

$$\int_0^{Z_1} O[x + B_{u,n}^0(a)] du \leq \int_0^{Z_1} O[x + B_{u,n}^0(a)]^2 du$$

and shows that the variance of the path estimating function is always smaller than that of the point estimating function. The actual decrease in the variance is not always significant because the points $x + B_{u,n}^0(a)$ for different u are strongly correlated. Depending on the nature of the function $O(x)$, the variance decrease may not compensate the effort required to compute the average $\int_0^{Z_1} O[x + B_{u,n}^0(a)] du$. However, if the function $O(x)$ is the potential $V(x)$, then the smaller variance of the path estimator is a desirable feature because the path average $\int_0^{Z_1} V[x + B_{u,n}^0(a)] du$, which also enters the expression of $X_n(x; a)$, is computed anyway.

To summarize the findings of the present subsection, the point estimator provides a more accurate value but has a larger variance than the path estimator. We next ask if there are any methods for which one may construct an estimator providing the same values as the point estimator but having the variance of the path estimator. More precisely, we seek methods for which there is a division $0 = u_0 < u_1 < \dots < u_{q_n} < u_{q_n+1} = 1$ such that the mesh $\max_{i \in [q_n, q_{n+1}]} |u_{i+1} - u_i|$ converges to zero as $n \rightarrow \infty$ and such that the points $x + B_{u_i,n}^0(a); 0 \leq i \leq q_n + 1$

have the same marginal distribution as x . For such methods, the expected value of the estimating function

$$\int_0^{Z_1} O[x + B_{u_i,n}^0(a)](u_{i+1} - u_i) du = 0 \quad (20)$$

under the probability distribution given by Eq. (19) is an estimator satisfying the criteria outlined in this paragraph.

There are two methods we employ in the present paper for which such an estimator exists. The first one, is the trapezoidal Trotter discrete path integral method (TT-DPI) obtained by the Trotter composition

$$\begin{aligned} \int_0^{Z_1} O(x; x^0; \cdot) dx_1 &= \int_0^{x_1} dx_1 \cdots \int_0^{x_n} dx_n \int_0^{x_n} O(x; x_1; \frac{x_n - x_1}{n+1}) \\ &\cdots \int_0^{x_1} O(x_n; x^0; \frac{x_n - x_1}{n+1}) \end{aligned} \quad (21)$$

of the short-time approximation

$$\int_0^{Z_1} O(x; x^0; \cdot) = f_p(x; x^0; \cdot) \exp \frac{V(x) + V(x^0)}{2} \cdot$$

It has been shown¹⁵ that for $n = 2^k - 1$, the TT-DPI method admits the following implementation

$$\begin{aligned} \frac{\int_0^{Z_1} O(x; x^0; \cdot) dx}{f_p(x; x^0; \cdot)} &= \int_0^{Z_1} da_{1,1} \cdots \int_0^{Z_1} da_{k,2^{k-1}} (2) \int_0^1 \exp \left(\frac{1}{2} \sum_{l=1}^k \sum_{i=1}^{2^{l-1}} a_{l,i}^2 A \right) \\ &\quad \times \exp \left(\sum_{i=0}^{2^k-1} V[x_r(u_i)] + \sum_{l=1}^k F_{1;[2^{l-1}u_i]+1}(u_i) a_{l;[2^{l-1}u_i]+1} \right) ; \end{aligned} \quad (22)$$

where $u_i = 2^{-k}i$ for $0 \leq i \leq 2^k$ and

$$V_i = \begin{cases} 2^{-(k+1)}; & \text{if } i \leq 0; 2^k g; \\ 2^{-k}; & \text{if } 1 \leq i \leq 2^k - 1; \end{cases}$$

The functions $F_{l;k}(u)$ are the so-called Schauder functions,¹⁶ the definitions of which are presented in the cited references. We leave it for the reader to use Eq. (21) and show that if $x = x^0$, then all the points $x + B_{u_i,n}^0(a)$ have identical marginal distribution given by the formula

$$\frac{\int_0^{Z_1} O(x; \cdot) dx}{\int_0^{Z_1} f_p(x; \cdot) dx} ;$$

In this case, the point and the path estimators produce

identical results for the ensemble average of a diagonal operator \hat{O}

$$\frac{\int_0^{Z_1} \int_0^{Z_1} O(x; \cdot) O(x) dx}{\int_0^{Z_1} \int_0^{Z_1} f_p(x; \cdot) f_p(x) dx} ;$$

At least for the ensemble average of the potential energy, one should always use the path estimator, which has smaller variance.

A second method for which there is an estimator giving the same values as the point estimator but having (asymptotically, as $n \rightarrow \infty$) the variance of the path estimator is the so-called Levy-Ciesielski reweighted technique (RW-LCP) defined by the formula⁴

$$\frac{\mathbb{E}^{\text{LC}}_n(\mathbf{x}; \mathbf{x}^0; \mathbf{a})}{\mathbb{E}^{\text{fp}}_n(\mathbf{x}; \mathbf{x}^0; \mathbf{a})} = \frac{\int_{\mathbb{R}}^{\mathbb{R}} \cdots \int_{\mathbb{R}}^{\mathbb{R}} da_1,1 \cdots da_{k+2,2^{k+1}}(2) \exp(\frac{1}{2} \sum_{l=1}^{2^k} \sum_{j=1}^{2^k} a_{l,j}^2 A_{l,j}^2) \exp \left(\sum_{l=1}^{2^k} \sum_{j=1}^{2^k} a_{l,[2^{l-1}u_j]+1} F_{l,[2^{l-1}u_j]+1}^{(n)}(u_j) du \right)}{2^{(4n+3)/2}} ; \quad (23)$$

where $[2^{l-1}u]$ is the integer part of $2^{l-1}u$. It has been shown that for $n = 2^k - 1$, the RW-LCPIM method can be put in the Trotter product form⁴

$$\frac{\mathbb{E}^{\text{LC}}_n(\mathbf{x}; \mathbf{x}^0; \mathbf{a})}{\mathbb{E}^{\text{fp}}_n(\mathbf{x}; \mathbf{x}^0; \mathbf{a})} = \frac{\int_{\mathbb{R}}^{\mathbb{R}} dx_1 \cdots \int_{\mathbb{R}}^{\mathbb{R}} dx_n \frac{\mathbb{E}^{\text{LC}}_0(\mathbf{x}; \mathbf{x}_1; \mathbf{a})}{\mathbb{E}^{\text{fp}}_0(\mathbf{x}; \mathbf{x}_1; \mathbf{a})} \cdots \frac{\mathbb{E}^{\text{LC}}_0(\mathbf{x}_n; \mathbf{x}^0; \mathbf{a})}{\mathbb{E}^{\text{fp}}_0(\mathbf{x}_n; \mathbf{x}^0; \mathbf{a})}}{2^{(4n+3)/2}} ; \quad (24)$$

where

$$\frac{\mathbb{E}^{\text{LC}}_0(\mathbf{x}; \mathbf{x}^0; \mathbf{a})}{\mathbb{E}^{\text{fp}}_0(\mathbf{x}; \mathbf{x}^0; \mathbf{a})} = \frac{1}{(2)^{3/2}} \int_{\mathbb{R}}^{\mathbb{R}} \int_{\mathbb{R}}^{\mathbb{R}} \int_{\mathbb{R}}^{\mathbb{R}} e^{(a_1^2 + a_2^2 + a_3^2)/2} \exp \left(\sum_{l=1}^{2^k} V[\mathbf{x} + (x^0 - \mathbf{x})u + a_1 C_0(u) + a_2 L_0(u) + a_3 R_0(u)] du \right) da_1 da_2 da_3 ;$$

The analytical expressions of the functions $F_{k,l}^{(n)}(u)$, $L_0(u)$, $R_0(u)$, and $C_0(u)$ can be found in Refs. (4) and (6).

Again, we leave it for the reader to use Eq. (24) and prove that if $\mathbf{x}^0 = \mathbf{x}$, then all the points

$$\mathbf{x} + \sum_{l=1}^{2^k} a_{l,[2^{l-1}u_i]+1} F_{l,[2^{l-1}u_i]+1}^{(n)}(u_i)$$

with $u_i = 2^{-k}i$ for $0 \leq i \leq 2^k$ have identical marginal distributions equal to that of \mathbf{x} . The estimator

$$\sum_{i=0}^{2^k} \sum_{l=1}^{2^k} \mathbf{x} + a_{l,[2^{l-1}u_i]+1} F_{l,[2^{l-1}u_i]+1}^{(n)}(u_i) \quad (25)$$

produces the same results as the point estimator, but it has the variance of the path estimator. As far as the evaluation of the average potential energy is concerned, in order to avoid unnecessary calls to the potential routine, it

is desirable that the points $f_{2^k} \leq i \leq 2^k$ be among the quadrature points utilized for the computation of the path averages appearing in Eq. (23). The quadrature technique designed in Ref. (6) shares this property. As opposed to the TT-DPII method, the point and the path estimators for the RW-LCPIM method produce different results.

B. Estimators for the total energy

In this subsection, we discuss the implementation of the thermodynamic (T) and the direct (H) estimators for the total energy. The T-m method estimator is defined as the following functional of the diagonal density matrix:

$$hE^T = \frac{1}{\mathbb{E}} \ln \int_{\mathbb{R}}^{\mathbb{R}} (\mathbf{x}; \mathbf{a}) dx ; \quad (26)$$

The above formula can be expressed as the statistical average

$$hE^T = \frac{\int_{\mathbb{R}}^{\mathbb{R}} dx \int_{\mathbb{R}}^{\mathbb{R}} dP[\mathbf{x}][\mathbf{x}](\mathbf{x}; \mathbf{a}; \mathbf{a}) E_1^T(\mathbf{x}; \mathbf{a}; \mathbf{a})}{\int_{\mathbb{R}}^{\mathbb{R}} dx dP[\mathbf{x}](\mathbf{x}; \mathbf{a}; \mathbf{a})} ; \quad (27)$$

where the T-m method estimating function $E_1^T(\mathbf{x}; \mathbf{a}; \mathbf{a})$ can be shown to be²

$$E_1^T(\mathbf{x}; \mathbf{a}; \mathbf{a}) = \frac{1}{2} + \int_0^{Z_1} V[\mathbf{x} + B_u^0(\mathbf{a})] du + \frac{1}{2} \int_0^{Z_1} V[\mathbf{x} + B_u^0(\mathbf{a})] B_u^0(\mathbf{a}) du \quad (28)$$

provided that $e^{-V(\mathbf{x})}$ has (Sobolev) first order derivatives as a function of \mathbf{x} . For a d-dimensional system, the expression of the T-m method estimating function reads

$$E_1^T(\mathbf{x}_1; \dots; \mathbf{x}_d; \mathbf{a}_1; \dots; \mathbf{a}_d) = \frac{d}{2} + \int_0^{Z_1} V[\mathbf{x}_1 + B_u^{0,1}(\mathbf{a}_1); \dots; \mathbf{x}_d + B_u^{0,d}(\mathbf{a}_d)] du + \frac{1}{2} \int_0^{Z_1} \frac{1}{\mathbb{E}[\mathbf{x}_i]} V[\mathbf{x}_1 + B_u^{0,1}(\mathbf{a}_1); \dots; \mathbf{x}_d + B_u^{0,d}(\mathbf{a}_d)] B_u^{0,i}(\mathbf{a}_i) du ; \quad (29)$$

The ensemble average energy can be obtained as the limit $n \rightarrow 1$ of the sequence

$$\text{HE}^T_{\text{m}} = \frac{\int_R dx \int_R dP \hat{a}X_n(x; a;) E_n^T(x; a;)}{\int_R dx \int_R dP \hat{a}X_n(x; a;)}, \quad (30)$$

where

$$E_n^T(x; a;) = \frac{1}{2} + \frac{Z_1}{V} x + \int_0^1 B_{u,n}^0(a) du + \frac{Z_1}{2} V^0 x + \int_0^1 B_{u,n}^0(a) B_{u,n}^0(a) du. \quad (31)$$

The finite-dimensional integral appearing in Eq. (30) can be evaluated by Monte Carlo integration. Because the temperature dependence of the Brownian bridge has been folded into the path average of the potential energy from the outset, the T-estimator produced by the present discussion emerges naturally in "virial" form.⁷ In the limit $n \rightarrow 1$, the variance of the estimator is finite because the square of $E_1^T(x; a;)$ given by Eq. (21) is a well-defined function, the average value of which is finite for smooth enough potentials.

A second energy estimator we employ in the present paper is the H-m method estimator. This direct estimator

is defined by the equation

$$\text{HE}^H = \frac{\int_R dx \int_R dP \hat{a}X_n(x; x^0;) E_n^H(x; a;)}{\int_R dx \int_R dP \hat{a}X_n(x; a;)}, \quad (32)$$

where the Hamiltonian of the system \hat{H}_{x^0} is assumed to act on the density matrix through the variable x^0 . By explicit computation and some integration by parts, the H-m method estimator can be expressed as the statistical average

$$\text{HE}^H = \frac{\int_R dx \int_R dP \hat{a}X_1(x; a;) E_1^H(x; a;)}{\int_R dx \int_R dP \hat{a}X_1(x; a;)} \quad (33)$$

of the estimating function²

$$E_1^H(x; a;) = \frac{1}{2} + V(x) + \frac{\int_0^2 Z_1}{4m_0} (u^2 - u^0)^2 + V^0[x + B_u^0(a)]V^0[x + B_u^0(a)] du d : \quad (34)$$

The H-estimator is properly defined even for potentials that do not have second-order derivatives. For a d-dimensional system, the H-m method estimating function reads

$$E_1^H(x_1; \dots; x_d; a_1; \dots; a_d;) = \frac{d}{2} + V(x_1; \dots; x_d) + \sum_{i=1}^{d-2} \frac{Z_1}{4m_0} (u^2 - u^0)^2 + \frac{\partial}{\partial x_i} V(x_1 + B_u^{0,1}(a_1); \dots; x_d + B_u^{0,d}(a_d)) + \frac{\partial}{\partial x_i} V(x_1 + B_u^{0,1}(a_1); \dots; x_d + B_u^{0,d}(a_d)) du d : \quad (35)$$

The reader should notice that the double integral appearing in Eq. (34) is really a sum of products of one-dimensional integrals. Indeed, one easily computes

$$E_1^H(x; a;) = \frac{1}{2} + V(x) + \frac{\int_0^2 u^2 V^0[x + B_u^0(a)] du}{2m_0} - \frac{\int_0^2 V^0[x + B_u^0(a)] du}{2m_0} + \frac{\int_0^2 u^2 V^0[x + B_u^0(a)] du}{2m_0} - \frac{\int_0^2 uV^0[x + B_u^0(a)] du}{2m_0} : \quad (36)$$

The H-m method estimator is the sum of the "classical" energy and a "quantum" correction term. Equation (33) shows that the total energy can also be recovered as the limit $n \rightarrow 1$ from the sequence

$$\text{HE}^H_{\text{m}} = \frac{\int_R dx \int_R dP \hat{a}X_n(x; a;) E_n^H(x; a;)}{\int_R dx \int_R dP \hat{a}X_n(x; a;)}, \quad (37)$$

where

$$E_n^H(x; a;) = \frac{1}{2} + V(x) + \frac{\int_0^2 Z_1}{4m_0} (u^2 - u^0)^2 + V^0[x + B_{u,n}^0(a)]V^0[x + B_{u,n}^0(a)] du d : \quad (38)$$

The forms of the T- and the H-m method estimators derived here with the reweighted techniques in mind extend naturally to the TT-DRIM method by means of Eq. (22). One just replaces the one-dimensional integrals appearing in Eqs. (31) and (38) by appropriate trapezoidal quadrature sums.

There is one special property of the T- and H-m method estimators that proves to be important in simulations. Let us notice that by virtue of the Boltzmann equation

$$\hat{H}_{x^0}(x; x^0;) = -\frac{\partial}{\partial x} (x; x^0;);$$

we have the equality

$$hE i \approx hE i^H = hE i^T :$$

However, since $\int_n^R H(x; x^0;) dx$ does not satisfy the Boltzmann equation (except for the free particle), in general

$$hE i_m^H = \frac{\int_R^R H(x; x^0;) \int_{x^0}^x dx}{\int_R^R Z(x;) dx}$$

$$hE i_m^T = \frac{\frac{\partial}{\partial} \ln \int_R^R Z(x;) dx}{\int_R^R Z(x;) dx}$$

and the T- and H-m method estimators produce the same result only in the limit $n \rightarrow 1$. Given that the two energy estimators discussed in the present section can be computed simultaneously without incurring any computational penalty, we recommend that the agreement between the T- and the H-m method estimators be used as a verification tool in actual simulations in order to check the convergence of various path integral methods.

As Eqs. (31) and (38) show, the path and the point estimating functions for the potential energy enter naturally the expressions of the T- and H-m method estimating functions, respectively. For the purpose of using the agreement between the two energy estimators as a verification tool for convergence, one should not replace the path estimating function for the potential energy in the expression of the T-m method estimator with the point estimating function, even if this may improve the estimated energy. For special cases, as for instance the TT-DPI and RW-LCPIM methods discussed in the previous subsection, one may replace the point estimating function for the potential energy appearing in the expression of the H-m method estimator with other estimating functions that produce the same value but have smaller variance. In this paper, we replace the point estimating function with the path estimating function for the TT-DPI method and with the estimating function given by Eq. (25) for the RW-LCPIM method, respectively.

III. A NUMERICAL EXAMPLE

We have tested the relative merits of the T- and H-m method energy estimators on a cluster of 22 hydrogen molecules at a temperature of 6 K, using three different path integral methods. Two of these methods, the trapezoidal Trotter discrete path integral method and a Levy-Ciesielski reweighted technique, have been already presented in the preceding section. The third method is a Wiener-Fourier reweighted (RW-WFP) technique introduced in Ref. (4). The numerical implementation of the methods has been extensively discussed in Ref. (6) by some of us and are not reviewed here.

The physical system we study has been recently examined by Chakravarty, Gordillo, and Ceperley¹⁰ as well as by Doli and Freeman¹¹ in their comparison of Fourier

and discrete path integral Monte Carlo methods. The total potential energy of the $(H_2)_{22}$ cluster is given by

$$V_{\text{tot}} = \sum_{i < j}^N V_{LJ}(r_{ij}) + \sum_{i=1}^N V_c(r_i); \quad (39)$$

where $V_{LJ}(r_{ij})$ is the pair interaction of Lennard-Jones potential

$$V_{LJ}(r_{ij}) = 4 \frac{\frac{12}{r_{ij}} - \frac{6}{r_{ij}}}{r_{ij}} \# \quad (40)$$

and $V_c(r_i)$ is the constraining potential

$$V_c(r_i) = \frac{\frac{1}{r_i} \frac{R_{cm}}{r_i}}{R_c} \# \quad (41)$$

The values of the Lennard-Jones parameters R_{LJ} and R_{cm} used are 2.96 Å and 34.2 K, respectively.¹⁰ R_{cm} is the coordinate of the center of mass of the cluster and is given by

$$R_{cm} = \frac{1}{N} \sum_{i=1}^N r_i \# \quad (42)$$

Finally, $R_c = 4 R_{LJ}$ is the constraining radius. The role of the constraining potential $V_c(r_i)$ is to prevent molecules from permanently leaving the cluster since the cluster in vacuum at any finite temperature is metastable with respect to evaporation.

The optimal choice of the parameter R_c for the constraining potential has been discussed in recent work.¹⁷ If R_c is taken to be too small, the properties of the system become sensitive to its choice, whereas large values of R_c can result in problems attaining an ergodic simulation. To facilitate comparisons, in the current work, R_c has been chosen to be identical to that used in Ref. (10). While this choice of constraining potential can induce ergodicity problems in calculations of fluctuation quantities like the heat capacity, we provide evidence below that the simulations in the current work are ergodic.

The three path integral methods we have employed utilize different numbers of path variables for a given index n . For instance, the TT-DPI n -th order approximation to the density matrix $\langle x; x^0; \rangle$ utilizes n path variables for each physical dimension, whereas $\langle x; x^0; \rangle$ and $\langle x; x^0; \rangle$ utilize $4n + 3$ and $4n$ path variables, respectively. To ensure fair comparison with respect to the number of path variables employed, we have tabulated the total number of variables n_v used for each physical dimension and not the index n .

A. Sampling strategy

We have discussed in Section II that the evaluation of the ensemble average of any observable eventually re-

duces to the evaluation of the average of a certain estimating function against the probability distribution

$$\frac{1}{R} \int_{-R}^R \frac{X_n(x; a)}{dx} dP[a] X_n(x; a) \quad (43)$$

or its multidimensional counterpart. This probability distribution can be sampled with the help of the Metropolis algorithm, which comprises the following steps.^{18,19} One initializes the imaginary-time paths in some fashion. Then, one attempts a trial move of the paths, which may involve changing several coordinates at a time. The displacement of the new paths is usually chosen to be relative to the old paths. To ensure ergodicity, one makes sure that all variables of the system are eventually moved in a cyclic or a random fashion. The proposed path is then accepted or rejected with a certain probability. The average value of the quantity of interest is computed by averaging the values of the corresponding estimating function evaluated at the current paths.

To establish some notation necessary for our discussion, for each vector $r_i = (x_i; y_i; z_i)$ denoting the physical coordinates of the particle i , we let $a_i = f_{a_{i,1}}; \dots; a_{i,n_v}$ be the collection of path variables associated with the respective particle. Each

$$a_{i,k} = a_{i,k}^x; a_{i,k}^y; a_{i,k}^z$$

is itself a three-dimensional vector whose components denote the k -th parameter of particle i for the x , y , and z coordinates, respectively. Going back to the description of the Metropolis algorithm, the full imaginary-time path has been initialized by choosing the physical coordinates r_i randomly in a sphere of radius R_c centered about origin. The path variables a_i have been initialized with zero.

Except for the Wiener-Fourier method with $n_v = 512$ ($n = 128$), we update the individual particles one at a time in a cyclic fashion. Each update of a particle consists of an attempt to move the physical coordinate r_i together with the first one quarter of the path variables a_i (that is, together with the variables $f_{a_{i,k}}; 1 \leq k \leq n_v/4$) followed by a separate attempt to move the rest of the path variables associated with the particle i . Both the physical coordinates and the path variables are moved in a cube centered about the old coordinates:

$$r_i^0 = r_i + r(2u - 1)$$

and

$$a_{i,k}^0 = a_{i,k} + a(2u - 1);$$

where the three components of u are independent uniformly distributed random numbers on the interval $[0; 1]$. Throughout our simulations, we have used the following maximum displacement values: $r = 0.26 \text{ \AA}$ and $a = 0.15$. The sampling technique employed guarantees an acceptance ratio between 30% and 70% for all methods studied and for $n_v = 256$.

Because the acceptance ratio drops below 20% for the Wiener-Fourier reweighted technique with $n_v = 512$, each most basic step of the previously described algorithm has been decomposed into two successive steps. The first step is decomposed into an attempt to move the physical coordinate r_i together with the first 1/8 of the path variables a_i , followed by an attempt to move the physical coordinate r_i together with the next 1/8 path variables a_i . The second step is decomposed in a similar fashion; half of the remaining variables have been moved in a first attempt and then the other half in a second attempt. This restores the overall acceptance ratio to about 33%. In fact, we have monitored separately the acceptance ratio for the four different steps necessary to update all the coordinates associated with a given particle and have made sure that the sampling is well balanced in the sense that the acceptance for each individual step is about 30% or larger.

As a counting device, we define a pass as the minimal set of Monte Carlo attempts over all variables in the system. A pass consists of $2^{12} = 4096$ basic steps for all simulations with $n_v = 256$. For the Wiener-Fourier reweighted technique with $n_v = 512$, a pass consists of $4^{12} = 4096$ basic attempted moves. One also defines a block as a computational unit made up of ten thousand passes.

B. Embarrassingly parallel computation

In order to achieve a statistical error of about 0.1 K/molecule for all computed energies, we have employed a large number of Monte Carlo passes (10.4 million) and we have divided the computation in 16 independent tasks (40 for the Wiener-Fourier reweighted method with $n_v = 512$) to be run in parallel. The Monte Carlo simulations are embarrassingly parallel provided that one can generate independent streams of uniformly distributed random numbers. In this situation, there is no need for communication among the different code replica running on different nodes, and the program is an ideal candidate for use on a distributed computing cluster. However, to be mathematically rigorous, it is necessary to ensure that all the communication needed is already buried in the independence of the streams of random numbers. This underlies the need for "good" parallel random number generators.

The Mersenne Twister (MT) is a fast serial pseudorandom number generating algorithm with a long period and good k -distribution properties.²⁰ Quite interestingly, the algorithm allows for the development of random number generators meeting certain user specifications. For instance, one may specify the period (which must be a Mersenne prime number, i.e., a prime number of the form $2^p - 1$), the word size, or the memory size. Given a specified period, one may still produce various algorithms which differ by their characteristic polynomials. The dynamic creation of distributed random number generators

is based on the hypothesis that M T random number generators having relatively prime characteristic polynomials produce highly independent streams of random numbers.²¹ Because the laws by which the numbers are generated are significantly different, it is very probable that the streams produced by the different generators are highly uncorrelated. In this paper, we have used the Dynamic Creator C-language library²² with the Mersenne number 2^{3217} . The library outputs streams of 32-bit integers, which are easy to convert into real numbers on the interval $[0;1]$. Different streams are identified by different identification numbers. The streams have been initialized once at the beginning of the simulation with different seeds.

Given the 16 streams of independent random numbers, the Monte Carlo simulation proceeds as follows. For each stream, one performs an independent simulation consisting of 65 blocks. These blocks are preceded by 13 equilibration blocks, which are needed to bring the system into probable configurations but do not contribute to the averages of the estimating functions. For the Wiener-Fourier reweighted method with $n_v = 512$, we use 40 independent streams of 25 blocks each, for a total of 10 million passes. The equilibration phase consists of 5 blocks for each stream. Ideally, the length of the individual streams should be chosen to be sufficiently large, that the averages of the computed property for different streams are independent and normally distributed, as dictated by the central limit theorem. This requirement is satisfied by all simulations we have performed.

We have collected individual averages for all blocks and streams and performed several statistical tests verifying the applicability of the central limit theorem as well as the independence between the block averages of same or different streams. Let $f_Z^0;1 \leq i \leq 16; 1 \leq j \leq 65$ denote the block-averages of the property Z for stream i and block j (the RW-WFP simulation for $n_v = 512$ has been analyzed in a similar fashion). Under the assumption that the size of the blocks is large enough so that the correlation between different block-averages is negligible and under the assumption that the block-averages for different streams are highly uncorrelated, the values $Z_{i;j}$ should have a Gaussian distribution centered around the average value

$$\bar{Z} = \frac{1}{16} \sum_{i=1}^{16} \sum_{j=1}^{65} Z_{i;j} \quad (44)$$

with variance

$$\sigma^2(Z) = \frac{1}{16} \sum_{i=1}^{16} \sum_{j=1}^{65} Z_{i;j}^2 - \bar{Z}^2 \quad (45)$$

The validity of this assumption can be verified with the help of the Shapiro-Wilk's normality test.²³ If the collection of samples $Z_{i;j}$ does not pass the test, it does not necessarily follow that the samples $Z_{i;j}$ are not independent, as their distribution is normal only if the size of the

blocks is sufficiently large. At a significance level of 5%, we do not reject the Gaussian distribution hypothesis for all computed average properties. To within the statistical significance of our calculations, the samples $Z_{i;j}$ can be assumed to be independent and have a Gaussian distribution.

A second set of tests consists in verifying that the row and column averages of $Z_{i;j}$ have Gaussian distributions centered around \bar{Z} with variances $\sigma^2(Z) = 65$ and $\sigma^2(Z) = 16$, respectively. The validity of this distribution follows from the central limit theorem and the assumption that the samples $Z_{i;j}$ are independent and have a Gaussian distribution characterized by the average \bar{Z} and the variance $\sigma^2(Z)$. It is important to emphasize that the row averages must pass this test. As previously discussed, the number of blocks in a stream should be sufficiently large so that the row averages have the required distribution even if the independent samples $Z_{i;j}$ do not have a Gaussian distribution. Again, under the assumption of independence only, the row averages should have a Gaussian distribution centered around \bar{Z} and have variance $\sigma^2(Z) = N_{\text{blocks}}$ for a sufficiently large number of blocks N_{blocks} . We have employed the Kolmogorov-Smirnov test²⁴ to compare the distributions of the row and column averages with the theoretical Gaussian distributions. For all computed average properties, we find that the respective distributions are identical at a statistical significance level of 5%. The agreement for the distribution of the row averages is evidence that the streams generated by the Dynamic Creator package are sufficiently independent, whereas the agreement for the distribution of the column averages is evidence that the block averages of the same streams are independent.

For the third set of tests, we have considered two time-series $f_Z^0;1 \leq i \leq 16 \leq 65$ and $f_Z^{20};1 \leq i \leq 16 \leq 65$ obtained by concatenating the rows of the matrix $Z_{i;j}$ and the columns, respectively. We then have studied the autocorrelation of the two time series for a maximum lag of 32. The correlation coefficients for a lag $k = 32$ are computed with the formula

$$r_k^0 = \frac{1}{\sigma^2(Z)} \frac{1}{16} \sum_{i=1}^{16} \sum_{j=1}^{65} Z_{i;j}^0 \bar{Z} - Z_{i+k}^0 \bar{Z} ;$$

where $Z_{i+k}^0 = Z_{i+k-16}^0 \dots Z_{i+k-65}^0$ if $i+k > 16 \leq 65$. Under the independence hypothesis of the samples Z_i^0 , the statistics of the correlation coefficients for $1 \leq k \leq 32$ is normal with average zero and standard deviation $\sigma^0 = \sqrt{\frac{1}{16} \sum_{i=1}^{16} \sum_{j=1}^{65} Z_{i;j}^2 - \bar{Z}^2}$. Moreover, the correlation coefficients can be regarded as independent samples of this normal distribution. By the binomial distribution, the probability that at most m correlation coefficients lie outside the interval $[-2\sigma^0, 2\sigma^0]$ is given by the formula

$$P(m) = \sum_{k=0}^m \frac{32!}{k!(32-k)!} q^k (1-q)^{32-k} ;$$

where $q = 0.046$ is the probability that a normal distributed variable of mean zero and standard deviation

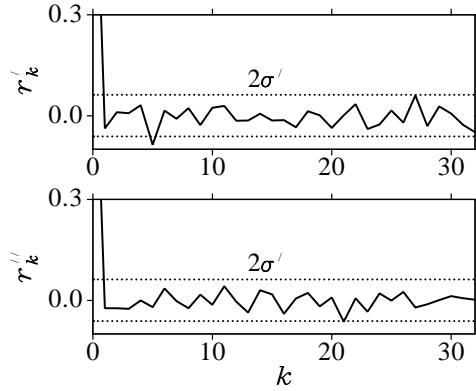


FIG. 1: Correlograms for the time-series Z_i^0 and Z_i^{00} . The property Z is the average ensemble energy computed by means of the H-m method estimator using the RW-W FPI method with $n_v = 32$. One notices that both the correlation between the block averages (r_k^0) and the correlation between the stream s (r_k^{00}) are negligible.

r_k^0 lies outside the interval $[-2^{-6}; 2^{-6}]$. One computes $P(3) = 0.942$ and $P(4) = 0.985$ so at a level of significance of 5%, the hypothesis that the r_k^0 are independent samples of a normally distributed variable of mean zero and standard deviation $\sigma = 1/\sqrt{16 \cdot 65} = 1/8$ should be rejected if 4 or more correlation coefficients lying outside the interval $[-2^{-6}; 2^{-6}]$ are observed.

The autocorrelation of the series Z_i^0 is representative of the correlation between the block averages of same stream s, whereas the autocorrelation of the time series Z_i^{00} is representative of the correlation between the blocks of similar rank corresponding to different stream s. Fig. 1 shows the correlograms of the two series for a RW-W FPI Monte Carlo simulation with $n_v = 32$. The computed property is the H-m method energy estimator. Both series Z_i^0 and Z_i^{00} have only one point lying outside the interval $[-2^{-6}; 2^{-6}]$. These points are r_5^0 and r_{21}^{00} , respectively (of course, the points $r_0^0 = r_0^{00} = 1$ are not counted). Consequently, the simulation passes our third statistical test. In fact, all the simulations performed have passed this statistical test for all computed properties. We conclude that the correlation between the block averages of same or different stream s is negligible. By the central limit theorem, the statistical error in the determination of the average of the property Z is

$$2(Z) = \sqrt{\frac{16}{65}}; \quad (46)$$

where $2(Z)$ is defined by Eq. (45). (For the statistical error, we employ the 2 value, corresponding to an interval of 95% confidence. The 5% probability that the results lie outside the confidence interval is chosen to agree with the level of significance of the statistical tests).

The analysis performed in the present subsection demonstrates that the stream s generated by the Dynamical Creator algorithm have negligible correlation at least for

our purposes.

A separate advantage in the use of independent streams is to overcome the phenomenon of quasiergodicity,²⁵ which might appear in Monte Carlo simulations whenever the distribution that is sampled has several well defined minima that are separated by walls of high energy. In this case, the random walker may be trapped in one of the wells and never sample the others, or sample them with the wrong frequency. The Monte Carlo simulation may pass all the aforementioned statistical tests but still produce the wrong results. For our system, the probability that such a situation may occur is quite low because the system is highly quantum mechanical with strong barrier tunneling. Moreover, the 16 independent streams have been initialized randomly in configuration space. This makes it unlikely that all the streams are trapped precisely into the same local minimum or group of local minima. Evidence for quasiergodicity may be captured in the form of a few outlying averages among the stream averages. Such outlying averages have not been observed.

C. Summary and discussion of the computed averages

The computed averages for all methods and estimators utilized are presented in Tables I, II, and III. For a given number of path variables n_v , the RW-W FPI, RW-LCP I, and TT-DPI methods utilize $2n_v$, $2.25n_v$, and n_v quadrature points, respectively. [For a discussion of the minimal number of quadrature points and of the nature of the quadrature schemes that must be employed for the first two methods, the reader should consult Ref. (6). For the RW-W FPI method, we have utilized $2n_v$ Gauss-Legendre quadrature points, though a number of $1.75n_v$ points would have sufficed.] The observed overall computational time for the three methods have followed the ratios $2:2.25:1$, even though the time necessary to compute the paths is proportional to n_v^2 for the first method and to $n_v \log_2(n_v)$ for the other methods. The computation of the paths takes full advantage of the vector floating point units of the modern processors and is dominated by the calls to the potential, except for very large n_v .

As discussed in Ref. (6), the asymptotic convergence for the few weighted techniques is expected to be cubic, even for the Lennard-Jones potential that is not included in the class of potentials for which cubic convergence has been demonstrated formally. We find that the asymptotic convergence is attained only for very large n_v , as one may see by comparing for example the total, potential, and kinetic energies computed with the help of the T-m method estimator for the RW-LCP I and the TT-DPI methods. Even if the latter method has only $1=n_v^2$ asymptotic convergence, the two methods produce almost equal

results. In fact, a numerical analysis of the relationship

$$\text{HE i}^T_{n_v} = \text{HE i} + \frac{\text{const.}}{(n_v)};$$

in which the left-hand side quantity is plotted against $1/(n_v)$ for different values of n_v , suggests that, while the methods have converged within the statistical error, none of the three methods includes sufficiently large values of n_v to attain the ultimate asymptotic rate of convergence.

When comparing the values of the H_m method energy estimator and of the related potential and kinetic estimators for the three path integral techniques, one notices that the RW-LCP I technique provides better values than the TT-DPI method. The H_m method estimator has a better behavior if used together with a reweighted technique. This behavior is consistent with the analysis we have performed in Section II on the values of the potential-point-estimators and the excellent values found with the RW-WFPI method. For the reweighted techniques, the H_m method estimator provides better energy values than the T_m method estimator. This is also true of the potential and kinetic parts of the estimators. However, the variance of the H_m method estimator is significantly larger than the variance of the T_m method estimator and the difference is even more pronounced if one compares the corresponding kinetic estimators.

Among the three methods presented, the RW-WFPI has the fastest convergence for all properties studied. Moreover, for $n_v = 128$ and $n_v = 256$, there is a good agreement (within statistical noise) between the T - and the H_m method energy estimators, as well as between their potential and kinetic energy components. For $n_v = 256$, one concludes that the systematic error is smaller than the statistical error for all properties computed. An additional RW-WFPI simulation with $n_v = 512$ has produced results consistent with the findings above. We report as our best energy estimates the averages between the energies computed with the RW-WFPI technique for $n_v = 256$ and $n_v = 512$. These averages are summarized in Table IV.

IV. CONCLUSIONS

In the present work we have considered a number of issues related to the choice of estimators for random series path integral methods. We have illustrated our results by applying them to the problem of computing various thermodynamic properties of a model of the $(H_2)_{22}$ cluster using reweighted path integral techniques. The molecular hydrogen cluster is a strongly quantum mechanical system and is representative of the type of problems one is likely to encounter in many applications. Hence, it constitutes a useful benchmark for present and future path integral techniques and for this reason it is important that its physical properties be determined within advertised statistical error bars. Path integral methods capable of dealing with such highly quantum mechanical

systems in an efficient manner are needed, both for reliable determinations of the physical properties of the respective systems as well as for accurate parameterizations of the intermolecular potentials.

We wish to make a number of points concerning the present results and the methods we have utilized to obtain them. At a more general level, we would like to emphasize that the reweighted path integral methods discussed here provide a broadly applicable, simple, and formally well characterized set of techniques. As demonstrated by the present results, they are capable of producing high-quality numerical results for problems of appreciable physical complexity. Moreover, they do so without the assumption of a particular form for the underlying microscopic forces. Furthermore, the estimators described in the present paper are convenient, accurate, and easily implemented for any random series approach. As discussed in Section III, when used together, the T and H_m method estimators provide an important consistency check on the quality of the path integral simulations. Such consistency checks are a valuable element in judging the reliability of particular simulations.

As previously mentioned, the cluster application discussed here provides a convenient test bed for the development of numerical methods. For this reason, we have exercised due diligence with respect to the quality of our final results summarized in Table IV. As discussed in Section III, we have subjected both the parallel random number generator employed and the numerical results obtained to a series of quality-control tests. Beyond these statistical checks, it is important to note there is an internal consistency check on the quality of the present results. Specifically, as is evident in Tables I, II, and III, the kinetic, potential, and total energies from the three different path integral approaches (trapezoidal Trotter, reweighted Levy-Ciesielski, and reweighted Wiener-Fourier) all agree. It is also important to note in this context that, while the presently computed total energies agree with those reported by Chakravarty et al.,¹⁰ the individual kinetic and potential energies do not. The kinetic energy reported by Chakravarty et al.¹⁰ is approximately 0.8 K/particle higher than found in the present simulations (with the potential energy being correspondingly lower). The magnitude of this difference is well outside the statistical error bars involved and appears to signal a systematic error. Based on the observed consistency between the results produced by three different path integral methods and on the agreement between the T and H_m method estimators for each of these path integral formulations, we feel confident of the results we have reported in Table IV.

Note: After the present simulation has been completed, we have learned from D. M. Ceperley that the off-diagonal pair density used as the starting point in the simulations reported in Ref. (10) was truncated at first order in the expansion of off-diagonal displacements instead of second order and that the inclusion of this second order term resolves the kinetic and potential energy

difference noted above.

Acknowledgments

The authors acknowledge support from the National Science Foundation through awards No. CHE-0095053 and CIE-0131114. They also wish to thank the Center for Advanced Scientific Computing and Visualization (TCA SCV) at Brown University for valuable assistance with respect to the numerical simulations described in the present paper. They would also like to thank Mr. Cristian Diaconu for helpful discussions concerning the present work. Finally, the authors would like to express a special thanks to Professor David Ceperley for continuing discussions concerning the present simulations

and for his efforts in tracking down the origin of the pair density issues noted in Section IV.

APPENDIX A

The main purpose of this section is to give a compact form for the integral

$$\int_0^1 dP_B \mathbb{E}[X_1(x; x^0; a;)O[x_r() + B^0(a)]; (A1)$$

where x is an arbitrary point in the interval $[0; 1]$. In terms of a standard Brownian motion [see Eq. (1)], the above integral can be put into the form

$$\begin{aligned} P_B B_1 &= x^0 B_0 = x \int_0^1 e^{\int_0^1 V(B_u) du} O(B) B_1 = x^0; B_0 = x \\ &= \int_0^1 dy O(y) P_B B_1 = x^0; B = y B_0 = x \int_0^1 e^{\int_0^1 V(B_u) du} B_1 = x^0; B = y; B_0 = x : \end{aligned} \quad (A2)$$

Using the Markov property of the Brownian motion, one readily justifies the equalities

$$\begin{aligned} P_B B_1 &= x^0; B = y B_0 = x \\ &= P_B B_1 = x^0 B = y P_B = y B_0 = x \quad (A3) \\ &= f_P(x; y;) f_P(y; x^0; (1 -)) \end{aligned}$$

and

$$\begin{aligned} &\int_0^1 e^{\int_0^1 V(B_u) du} B_1 = x^0; B = y; B_0 = x \\ &= \int_0^1 e^{\int_0^1 V(B_u) du} B = y; B_0 = x \quad (A4) \\ &= \int_0^1 e^{\int_0^1 V(B_u) du} B_1 = x^0; B = y : \end{aligned}$$

Performing the transformation of coordinates $u^0 = u$ in the second factor of the right-hand side of Eq. (A4) and employing the invariance of the Brownian motion under time translation

$$\begin{aligned} B_{u+} B = y; B_1 &= x^0; u = 0 \\ &= B_u B_0 = y; B_1 = x^0; u = 0 ; \end{aligned}$$

one obtains

$$\begin{aligned} &\int_0^1 e^{\int_0^1 V(B_u) du} B_1 = x^0; B = y; B_0 = x \\ &= \int_0^1 e^{\int_0^1 V(B_u) du} B = y; B_0 = x \quad (A5) \\ &= \int_0^1 e^{\int_0^1 V(B_u) du} B_1 = x^0; B_0 = y : \end{aligned}$$

Let us focus on the term

$$\int_0^1 e^{\int_0^1 V(B_u) du} B = y; B_0 = x :$$

Performing the substitution of variables $u^0 = u =$ and employing the scaling property of the Brownian motion

$$\begin{aligned} &\int_0^1 e^{\int_0^1 V(B_u) du} B_0 = x; B = y; u = 0 \\ &\stackrel{d}{=} \int_0^1 e^{\int_0^1 V(B_u) du} B_0 = x; B_1 = y; u = 0 ; \end{aligned}$$

one proves

$$\begin{aligned} &\int_0^1 e^{\int_0^1 V(B_u) du} B = y; B_0 = x \\ &= \int_0^1 e^{\int_0^1 V(B_u) du} B_1 = y; B_0 = x \quad (A6) \\ &= (x; y;) = f_P(x; y;) : \end{aligned}$$

In a similar fashion, one demonstrates that

$$\begin{aligned} &\int_0^1 e^{\int_0^1 V(B_u) du} B_1 = x^0; B_0 = y \\ &= (y; x^0; (1 -)) = f_P(y; x^0; (1 -)) : \end{aligned} \quad (A7)$$

We now combine Eqs. (A1), (A2), (A3), (A5), (A6), and (A7) to obtain

$$\begin{aligned} &\int_0^1 dP_B \mathbb{E}[X_1(x; x^0; a;)O[x_r() + B^0(a)] \\ &= (x; y;) (y; x^0; (1 -)) O(y) dy : \end{aligned} \quad (A8)$$

With the help of Eq. (A 8) and by cyclic invariance,

$$\begin{aligned}
 & \int_{\mathbb{R}^Z} dx \int_{\mathbb{R}^Z} dy \mathbb{P}[\mathbb{X}_1(x; a;)O(x + B^0(a))] \\
 &= \int_{\mathbb{R}^Z} dx \int_{\mathbb{R}^Z} dy (x; y;) [y; x; (1 -)] O(y) \\
 &= \int_{\mathbb{R}^Z} dy (y; y;) O(y) \\
 &= \int_{\mathbb{R}^Z} dx \int_{\mathbb{R}^Z} dy \mathbb{P}[\mathbb{X}_1(x; a;)O(x)];
 \end{aligned} \tag{A 9}$$

Moreover, since the function $O(x)$ is arbitrary, the last identity also implies that the random variables x and $x + B^0(a)$ have identical distribution functions under the probability measure

$$\int_{\mathbb{R}^Z} \frac{\mathbb{X}_1(x; a;) dx d\mathbb{P}[\mathbb{P}]}{\int_{\mathbb{R}^Z} dx d\mathbb{P}[\mathbb{X}_1(x; a;)]}:$$

By setting $O(x) = 1$ in Eq. (A 8), one obtains the well-known product formula

$$\begin{aligned}
 & \int_{\mathbb{R}^Z} (x; x^0;) = \int_{\mathbb{R}^Z} dx \int_{\mathbb{R}^Z} dy (x; y;) [y; x^0; (1 -)] dy;
 \end{aligned} \tag{A 10}$$

which is seen to be a consequence of some basic properties of the Brownian motion.

¹ Quantum Monte Carlo Methods in Physics and Chemistry, edited by M. P. Nightingale and C. J. Umrigar, (Kluwer, Dordrecht, 1999).

² C. Predescu and J. D. Doll, *J. Chem. Phys.* 117, 7448 (2002).

³ C. Predescu, J. D. Doll, and David L. Freeman, A sympathetic convergence of the partial averaging technique, e-print: <http://arxiv.org/abs/cond-mat/0301525>.

⁴ C. Predescu, Reweighted M methods: Definition and A sympathetic Convergence, e-print: <http://arxiv.org/abs/cond-mat/0302171>.

⁵ J. D. Doll, R. D. Coalson, and D. L. Freeman, *Phys. Rev. Letts.* 55, 1 (1985); R. D. Coalson, D. L. Freeman, and J. D. Doll, *J. Chem. Phys.* 85, 4567 (1986).

⁶ C. Predescu, D. Sabo, and J. D. Doll, Numerical implementation of some reweighted path integral techniques, e-print: <http://arxiv.org/abs/cond-mat/0305436>.

⁷ M. Eleftheriou, J. D. Doll, E. Curotto, and D. L. Freeman, *J. Chem. Phys.* 110, 6657 (1999).

⁸ M. F. Herman, E. J. Burskin, and B. J. Berne, *J. Chem. Phys.* 76, 5051 (1982).

⁹ D. M. Ceperley, *Rev. Mod. Phys.*, 67, 279 (1995).

¹⁰ C. Chakravarty, M. C. G. Ordillo, and D. M. Ceperley, *J. Chem. Phys.* 109, 2123 (1998).

¹¹ D. Doll and David L. Freeman, *J. Chem. Phys.* 111, 7685 (1999).

¹² B. Simon, Functional Integration and Quantum Physics (Academic, London, 1979).

¹³ R. Durrett, Probability: Theory and Examples, 2nd ed.

Duxbury, New York, 1996), pp. 430-431.

¹⁴ S. Kwapień and W. A. Woyczyński, *Random Series and Stochastic Integrals: Single and Multiple* (Birkhäuser, Boston, 1992), Theorem 2.5.1.

¹⁵ C. Predescu and J. D. Doll, *Phys. Rev. E* 67, 026124 (2003).

¹⁶ H. P. McKean Jr., *Stochastic Integrals* (Academic, New York, 1969).

¹⁷ J. P. Neirotti, D. L. Freeman, and J. D. Doll, *Phys. Rev. E* 62, 7445 (2000).

¹⁸ N. Metropolis, A. W. Rosenbluth, M. N. Rosenbluth, A. M. Teller, and E. Teller, *J. Chem. Phys.* 21, 1087 (1953).

¹⁹ M. Kalos and P. W. Hirsch, *Monte Carlo Methods* (Wiley-Interscience, New York, 1986).

²⁰ M. Matsumoto and T. Nishimura, *ACM Transactions on Modeling and Computer Simulation* 8, 3 (1998).

²¹ M. Matsumoto and T. Nishimura, *Dynamic Creation of Pseudorandom Number Generators*, in *Monte Carlo and Quasi-Monte Carlo Methods 1998*, (Springer-Verlag, New York, 2000), pp. 56-69.

²² <http://www.math.keio.ac.jp/~matumoto/emt.html>.

²³ S. S. Shapiro and M. B. Wilk, *Biometrika*, 52, 591 (1965).

²⁴ W. H. Press, S. A. Teukolsky, W. T. Vetterling, and B. P. Flannery, *Numerical Recipes* (Cambridge University, Cambridge, 1992) Ch. 14.3.

²⁵ J. P. Valleau and S. G. Whittington, in *Statistical Mechanics*, edited by B. J. Berne (Plenum, New York, 1977) Ch. 4, p. 145.

TABLE I: Listed are the results obtained by the Wiener-Fourier reweighted path integral method. Average potential $\langle hV \rangle^T$, kinetic $\langle hK \rangle^T$, and total energies $\langle hE \rangle^T$ are calculated with the help of the T- and H-estimators as functions of the number of path variables n_v . The error bars are two standard deviation values. All energies are given in K/m molecule.

n_v	$\langle hE \rangle^T$		$\langle hE \rangle^H$		$\langle hV \rangle^T$		$\langle hV \rangle^H$		$\langle hK \rangle^T$		$\langle hK \rangle^H$	
4	-57.66	0.05	-16.63	0.18	-82.14	0.07	-61.72	0.12	24.48	0.02	45.09	0.15
8	-37.61	0.05	-17.77	0.16	-64.74	0.06	-53.07	0.11	27.13	0.02	35.29	0.13
16	-25.68	0.04	-18.28	0.13	-54.27	0.06	-49.33	0.10	28.60	0.03	31.06	0.11
32	-20.23	0.04	-18.00	0.12	-49.66	0.06	-48.05	0.10	29.42	0.03	30.05	0.11
64	-18.29	0.04	-17.85	0.11	-48.19	0.06	-47.86	0.09	29.90	0.03	30.01	0.11
128	-17.75	0.04	-17.64	0.12	-47.83	0.06	-47.81	0.09	30.08	0.03	30.17	0.11
256	-17.71	0.04	-17.70	0.12	-47.85	0.07	-47.87	0.10	30.14	0.03	30.17	0.12
512	-17.68	0.04	-17.81	0.11	-47.81	0.06	-47.90	0.09	30.13	0.03	30.10	0.10

TABLE II: Listed are the results obtained by the Levy-Ciesielski reweighted path integral method. The format is that of Table I.

n_v	$\langle hE \rangle^T$		$\langle hE \rangle^H$		$\langle hV \rangle^T$		$\langle hV \rangle^H$		$\langle hK \rangle^T$		$\langle hK \rangle^H$	
3	-70.46	0.06	18.24	0.20	-93.47	0.07	-69.03	0.09	23.01	0.02	87.27	0.19
7	-44.08	0.05	-10.81	0.15	-71.03	0.06	-55.08	0.08	26.94	0.02	44.28	0.14
15	-29.84	0.04	-15.84	0.12	-58.33	0.06	-49.10	0.07	28.50	0.02	33.26	0.12
31	-22.76	0.04	-17.40	0.10	-51.95	0.06	-47.83	0.06	29.19	0.03	30.43	0.11
63	-19.50	0.04	-17.68	0.10	-49.15	0.06	-47.69	0.06	29.65	0.03	30.01	0.11
127	-18.25	0.04	-17.68	0.10	-48.20	0.06	-47.80	0.06	29.95	0.03	30.11	0.11
255	-17.84	0.04	-17.65	0.11	-47.93	0.07	-47.85	0.07	30.09	0.03	30.20	0.12

TABLE III: Listed are the results obtained by the trapezoidal Trotter discrete path integral method. The format is that of Table I.

n_v	$\langle hE \rangle^T$		$\langle hE \rangle^H$		$\langle hV \rangle^T$		$\langle hV \rangle^H$		$\langle hK \rangle^T$		$\langle hK \rangle^H$	
3	-68.54	0.05	78.08	0.30	-89.88	0.07	-89.88	0.07	21.34	0.02	167.97	0.32
7	-45.29	0.05	7.22	0.19	-70.88	0.06	-70.88	0.06	25.58	0.02	78.10	0.21
15	-30.61	0.04	-12.52	0.13	-58.53	0.06	-58.53	0.06	27.92	0.02	46.01	0.15
31	-22.95	0.04	-16.86	0.11	-51.99	0.06	-51.99	0.06	29.04	0.03	35.14	0.12
63	-19.55	0.04	-17.66	0.10	-49.19	0.06	-49.19	0.06	29.65	0.03	31.53	0.11
127	-18.29	0.04	-17.70	0.10	-48.27	0.06	-48.27	0.06	29.97	0.03	30.57	0.11
255	-17.86	0.04	-17.71	0.11	-47.94	0.07	-47.94	0.07	30.07	0.03	30.23	0.12

TABLE IV : Estimated energies in K /m olecule for the $(H_2)_{22}$ cluster. Listed are the average potential hV_i^T , kinetic hK_i^T , and total energies hE_i^T calculated with the help of the T-m method (left column) and H-m method (right column) estimators. The reported errors are two standard deviations.

hE_i^T	17.70	0.04	hE_i^H	17.75	0.11
hV_i^T	47.83	0.06	hV_i^H	47.88	0.09
hK_i^T	30.13	0.03	hK_i^H	30.13	0.11